Spectrochimica Acta Part A: Molecular and Biomolecular Spectroscopy 226 (2020) 117650

Contents lists available at ScienceDirect

Spectrochimica Acta Part A: Molecular and Biomolecular Spectroscopy

journal homepage: www.elsevier.com/locate/saa

A facile AIE fluorescent probe for broad range of pH detection

Xiaoju Wang [a, 1], Haoping Wang [b, 1], Yan Niu [b], Yunxia Wang [b, **], Liheng Feng [b, *]

[a] Institute of Molecular Science, Chemical Biology and Molecular Engineering, Laboratory of Education Ministry, Shanxi University, Taiyuan, 030006, PR China

[b] School of Chemistry and Chemical Engineering, Shanxi University, Taiyuan, 030006, PR China

ARTICLE INFO

Article history:
Received 4 September 2019
Received in revised form
5 October 2019
Accepted 9 October 2019
Available online 12 October 2019

Keywords:
Fluorescent dye
pH detection
Aggregation-induced emission
Coumarin
Quinoline

ABSTRACT

Detection of pH has received more and more attention in various fields. Currently, a hot research topic is focused on how to use a facile fluorescent dye to achieve a wide range and accurate pH detection. Herein, we reported a simple fluorescence probe for pH detection with wide range and accuracy based on the Aggregation-Induced Emission (AIE) characteristics. The probe 2-oxo-N'-(2-(quinolin-8-yloxy)acetyl)-2H-chromene-3-carbo- hydrazide (CHBQ) as comprised of coumarin and quinoline as the electron donor and acceptor, N, N′-diformylhydrazine bond as the linking group, respectively. The probe displays good AIE characteristics under water content up to 99% in mixed medium. Furthermore, it can identify acid and base as fast as 30 s by color change of the solution under $UV_{365\ nm}$ lamp. The detection of the probe for pH was hardly interfered with other ions. What's more, the probe CHBQ can be designed to be a broad range test paper of pH detection, which has a great practical value.

1. Introduction

PH is an important parameter in many fields. The determination of waste water pH [1–3], soil pH [4–6], drug pH [7], and food pH [8] is of great significance for the field of industry, agriculture, medicine and food safety inspection. Therefore, the rapid detection and monitor of pH changes is meaningful. On account of that fluorescence analysis technology has the characteristics of high sensitivity, fast response times, high signal-to-noise ratio, and continuous dynamic monitors [9–11], fluorescent probes for pH detection are developed rapidly. However, many of the pH fluorescence probes reported so far monitored pH with the range of about 2.00–7.00 [12–16] and only a few probes are able to detect fluorescence changes in alkaline environment [7,17]. Notably, the pH of some samples in the actual detection are in a broad range, which makes that probes with limited detection range invalid, and multiple detection methods are needed to achieve the purpose of pH detection. Therefore, it is necessary to develop a fluorescent pH probe for the detection of broad range pH. More importantly, the pH probes could response to acids and alkalis with different fluorescence signal under a single light resource is also scarce and deserved to be investigated and synthesized.

In general, most organic fluorescent probes are organic molecules that have poor solubility and luminescence in aqueous solutions owing to the aggregation caused quenching (ACQ) effect [18–22]. Therefore, for the detection of actual pH, molecules with Aggregation-Induced Emission (AIE) effect are attractive [23–25]. The AIE molecules discovered by professor Tang and his coworkers exhibited good photophysical properties in aqueous solution, and have been applied in many fields [23]. Different from traditional fluorescent molecules, AIE molecules could rotate randomly in organic solvents and resulting in a weak fluorescence. When in water systems, the rotation of AIE molecules is blocked and molecule rigidity is increased, leading to strong fluorescence of molecule [26–28]. The unique properties of the AIE molecules allow the detection only performed in organic solvents to be achieved in water systems. Some fluorescence probes that respond to pH composed of N-containing groups, such as pyridine [29–31], quinolone [32–34] and piperazine [35,36] etc. Due to the presence of lone pair electrons on the N atom, these groups can provide the binding site with H^+, so as to achieve the purpose of detecting H^+ by causing changes in fluorescence of the probe. In the Schiff base AIE molecule [37–40], the presence of -C=N group provides a potential pH sensing site. In view of that there is a tautomerism presented in N, N′-diformylhydrazine molecule in different polarity solvents, which is similar to the enol conversion of the ketone [41,42]. We combined the properties of the pH sensing group with

* Corresponding author.
** Corresponding author.
E-mail addresses: wangyunxia@sxu.edu.cn (Y. Wang), lhfeng@sxu.edu.cn (L. Feng).

[1] The authors of Xiaoju Wang and Haoping Wang contributed equally to this work.

https://doi.org/10.1016/j.saa.2019.117650
1386-1425/

the AIE molecules to design a pH-response AIE fluorescence probe. By utilizing coumarin and quinoline as electron donors and electron acceptors respectively, N, N′-diformylhydrazine bond as the linkage, a novel pH-responsive fluorescent probe CHBQ with AIE effect for the broad range pH detection have been synthesized successfully.

The synthesized probe CHBQ exhibited good AIE characteristics. In a mixed solvent of acetonitrile and water, the fluorescence located at 415 nm gradually increased with the increase of water proportion. In addition, a different fluorescence response could be observed in the presence of acids and bases. Under acidic conditions, the fluorescence emission peak of the probe CHBQ gradually decreased and generated blue shift from 475 nm to 415 nm with the pH changed from 2.00 to 6.00 and the color of solution changed from cyan to blue under $UV_{365\ nm}$ lamp. Under alkaline conditions, as the pH gradually increased, the fluorescence at 415 nm was decreased, and the blue color of the solution gradually became darkened under $UV_{365\ nm}$ lamp. Furthermore, the response time of probe CHBQ towards pH was extremely short as 30 s, rapid recognition of acid and base could be realized and almost impervious to other ions, such as some metal cations and anions. Finally, the probe CHBQ could be developed as a pH test strip to achieve a faster detection of a broad range pH in the actual sample.

2. Experimental

2.1. Materials and instruments

Unless otherwise stated, all chemical reagents were obtained from commercial suppliers and used without further purification. 4-Dimethylaminopyridine (DMAP), N,N′-dicyclohexylcarbodiimide (DCC), N-hydroxysuccinimide (NHS), Coumarin-3-Carboxylic acid, 8-hydroxyquinoline, and methanol (HPLC) were purchased from Energy Chemical (Shanghai, China) without any further purification. Metal ions were all nitrates salts, and anions were all sodium salt. All the salts were provided from Alfa Aesar (Tianjin, China). Hydrogen nuclear magnetic resonance (^{1}H NMR) and carbon nuclear magnetic resonance (^{13}C NMR) spectra were recorded on Bruker ARX600 and Bruker ARX400 spectrometer. Chemical shifts for hydrogens are reported as ppm (tetramethylsilane as an internal standard) and are referenced to the residual protons in the NMR spectra (DMSO: δ 2.50). ^{13}C NMR spectra were recorded at 100 MHz. Chemical shifts for carbons are reported as ppm (tetramethylsilane as an internal standard) and are referenced to the carbon resonance of the solvent (DMSO: δ 39.5). High Resolution Liquid Chromatography Mass Spectra (HPLC-MS) were acquired on Thermo Scientific Q Exactive instrument (Thermo Fisher Scientific, USA), which equipped with an electroscope ionization (ESI) source. UV-vis spectra were measured on Hitachi 5300 absorption spectrophotometer in a cuvette (1 cm in diameter) with 2 mL solution. Fluorescence spectra were recorded on Hitachi F-4600 fluorescence spectrophotometer using an excitation wavelength of 330 nm, and the excitation slit widths was 5 nm and emission slit widths was 10 nm, respectively. The pH value of solution was measured and controlled with a PHS-3C pH meter (Shanghai LeiCi Device Works, China). Density functional theory (DFT) (B3LYP/6-31G (d) level of theory) was utilized to model the structure geometry and electronic properties of relevant molecular.

2.2. Synthesis

The intermediate compounds of ethyl 2-(quinolin-8-yloxy)acetate and 2-(quinolin-8-yloxy) acetohydrazide (QA) were synthesized according to the previously reported reference [43]. A mixture of coumarin-3-carboxylic acid (0.57 g, 3.0 mmol), N-hydroxysuccinimide (NHS) (0.37 g, 3.2 mmol) and dicyclohexylcarbodiimide (DCC) (0.68 g, 3.3 mmol) in of DMF (8 mL) were stirred for about 8 h at room temperature. After filtration, the filtrate was added to the mixture solvent (50 mL) of isopropanol-hexane mixture (1/20) to obtain the intermediate 2,5-dioxopyrrolidin-1-yl-2-oxo-2H-chromene-3- carboxylate (DC) [44]. Next, the mixture of the intermediate DC, QA (0.70 g, 3.2 mmol) and 4-Dimethylaminopyridine (0.39 g, 3.2 mmol) in of DMF (10 mL) were reacted at 85 °C for 24 h. Then, pour the mixture into deionized water, extracting with dichloromethane. Collecting the organic phase, washed with saturated sodium chloride solution, and then dried by anhydrous sodium sulfate. The solvent was removed under reduced pressure to get crude product. The crude product was purified by column chromatography on silica gel with the eluent of methanol/dichloromethane (1/30, v/v) to obtained a pale yellow solid 2-oxo-N'-(2-(quinolin-8-yloxy)acetyl)-2H-chromene-3-carbohydrazide (CHBQ) 0.61 g, yield (52%). *^{1}H NMR (*600 MHz, *CH_3CN-d) δ (ppm): 11.72 (b, 1H), 10.82 (s, 1H), 9.00 (m, 1H,) 8.97 (s, 1H), 8.37 (d, J = 8.4* Hz, *1H), 7.97 (d, J = 7.8* Hz, *1H), 7.79 (m, 1H), 7.67 (d, J = 8.4* Hz *1H), 7.60 (m, 2H), 7.52 (d, J = 8.4* Hz, *1H), 7.48 (t, J = 7.2* Hz, *1H), 7.41 (d, J = 7.8* Hz, *1H), 4.99 (s, 4H); ^{13}C NMR (*100 MHz, *DMSO-d_6) δ (ppm) 165.87, 160.37, 159.04, 154.51, 154.45, 149.92, 148.56, 140.43, 136.59, 134.93, 130.87, 129.63, 127.27, 125.72, 122.51, 121.81, 118.80, 118.45, 116.74, 113.09, 68.70. HRMS-ESI calcd for $C_{21}H_{15}N_3O_5$ (m/z) $[M + H]^+$: 390.1084, found: 390.1085.*

2.3. Fluorescence and UV-Vis measurements

The stock solution of CHBQ (1.0×10^{-3} mol/L) was prepared in CH_3CN. In the pH response experiment, the pH meter was adjusted by using standard solution of potassium hydrogen phthalate (pH = 4.00) and mixed phosphate (pH = 6.86). Unless otherwise stated, the pH of the solution is adjusted by HCl and NaOH. In the interfering experiment, the pH = 4.00 buffer solution was prepared by dissolving potassium hydrogen phthalate in deionized water, and the pH = 9.18 buffer solution of was prepared by dissolving sodium tetrabrate in deionized water. The stock solutions of ions (1.0×10^{-2} mol/L) were prepared by dissolving them in deionized water. All of the experiments were performed at barometric pressure and room temperature. Excitation and emission slit widths was 5 nm and 10 nm, respectively.

2.4. Calculation of pKa

The pKa value was calculated by the Henderson-Hasselbach type mass action equation [45]: $pKa = pH - \log((F_{max}-F)/(F-F_{min}))$, where F is the fluorescence intensity of CHBQ at corresponding pH. F_{max} and F_{min} is minimal and maximal fluorescence intensity at detection range, respectively.

2.5. Preparation of test paper strips

The test paper strips were obtained by cutting filter paper with the size of 10 mm × 20 mm. Prepared filter paper was placed in acetonitrile solution of the CHBQ (2.0×10^{-3} mol/L), and dried in the air. Then 50 μL solutions of different pH were added to the filter paper. After placing the test paper 30 mm above the solvent and keeping it for 30s, the color of test paper above acetic acid and ethylenediamine changed to cyan and dark under UV365 nm lam, respectively The color changes of the test paper strips were observed under $UV_{365\ nm}$ lamps. In order to detect the fluorescence of the test paper discoloration, CHBQ was painted to the wall of the cuvette, and the fluorescence emission spectrum was recorded in different pH condition. The excitation wavelength was 330 nm, and the excitation and emission slits was 10 nm and 20 nm, respectively.

3. Results and discussion

3.1. Synthesis of probe CHBQ

The synthetic route of compound CHBQ is shown in Scheme S1. 8-Hydroxyquinoline was reacted with ethyl bromoacetate in the presence of potassium carbonate as the base in refluxed acetonitrile to afford ethyl 2-(quinolin-8-yloxy)acetate in 80% yield as a yellow oil, which was subsequently reacted with hydrazine hydrate in methanol at room temperature to afford 2-(quinolin-8-yloxy) acetohydrazide (QA) as a white solid. Coumarin 3-carboxylic acid was reacted with NHS in the presence of DCC at room temperature to get 2,5-dioxopyrrolidin-1-yl-2-oxo-2H-chromene-3-carboxylate (DC). Finally, compound DC was refluxed with compound QA in DMF for 24 h to give the final product CHBQ in 52% yield as pale yellow solid. Compound CHBQ was confirmed by conventional analytical methods, such as ^{1}H NMR (Fig. S1), ^{13}C NMR (Fig. S2), and ESI-MS (Fig. S3), respectively.

3.2. Photophysical properties of probe CHBQ

The photophysical properties of the probe CHBQ were studied in acetonitrile, water and solid state, respectively (Fig. 1a). When CHBQ (1×10^{-5} mol/L) is in acetonitrile solution, the absorption peaks of CHBQ is at 295 nm and 330 nm, and there is a weak fluorescence emission peak at about 405 nm. By contrast, when CHBQ is in aqueous solution (water content 99%), the absorption of CHBQ (1×10^{-5} mol/L) is at 300 nm and 335 nm, and the fluorescence emission peak is at about 415 nm. It can be seen that the absorption peak of CHBQ in water is a red shifted relative to that in acetonitrile, and the fluorescence is increased. While the absorption and maximum emission peaks of the CHBQ in solid are at 295 nm and 530 nm, respectively.

Interestingly, we found that the CHBQ exhibited AIE effect because it showed stronger fluorescence in water solution than that in acetonitrile. In the mixed solution of acetonitrile and water, the absorbance of probe CHBQ in 330 nm decreased gradually (Fig. S4) as increased volume of water. And the fluorescence of the probe CHBQ at about 415 nm increased (Fig. 1b), which could attributed to the aggregation of CHBQ in water.

In order to visualize the difference of CHBQ in different solvents and state, the photographs of CHBQ in CH_3CN, H_2O and solid state under sunlight and $UV_{365\ nm}$ lamp were shown in Fig. 1c. The color of CHBQ (5×10^{-4} mol/L) solution in CH_3CN was almost colorless and exhibited very weak blue fluorescence under sunlight and $UV_{365\ nm}$ lamp, respectively. The color of the CHBQ aqueous solution has little change under sunlight, but obvious blue fluorescence was observed under $UV_{365\ nm}$ lamp. Moreover, CHBQ solid is pale yellow solid and presents yellow fluorescence under sunlight and $UV_{365\ nm}$ lamp, respectively.

3.3. Optical response of the probe CHBQ to pH

In order to deeper understand the optical characteristics of the probe CHBQ, the pH response experiment was carried out by utilizing UV absorption spectrum and fluorescence emission spectrum in the mixed solution of acetonitrile/water (1/99, v/v). The absorption changes of the probe CHBQ (1×10^{-5} mol/L) at different pH were displayed in Fig. 2a. With the pH changes of the solution from 2.00 to 7.00, the shoulder absorption peak of CHBQ at 330 nm gradually weaken. Interestingly, the absorption peak at 330 nm is gradually redshift to 370 nm when the pH changes from 8.00 to 12.00. The change of fluorescence spectra of CHBQ in different pH were shown in Fig. 2b. When the pH of the solution changes from 2.00 to 6.00, the fluorescence of CHBQ at 475 nm decreases and generates blue shift from 475 nm to 415 nm. On the other hand, the fluorescence of CHBQ at 415 nm decreases gradually when the pH changes from 7.00 to 12.00. The result indicated that the probe CHBQ had an obvious fluorescence response to the change of pH. In addition, the acid titration and alkaline titration experiments were carried out to investigate the sensitivity of CHBQ for detecting pH. Nonlinear fit of the sigmoidal curve in acid and alkali (emission intensity versus pH value) afforded a pK_a value of 4.26 and 8.60 respectively. The fluorescence intensity value between the two

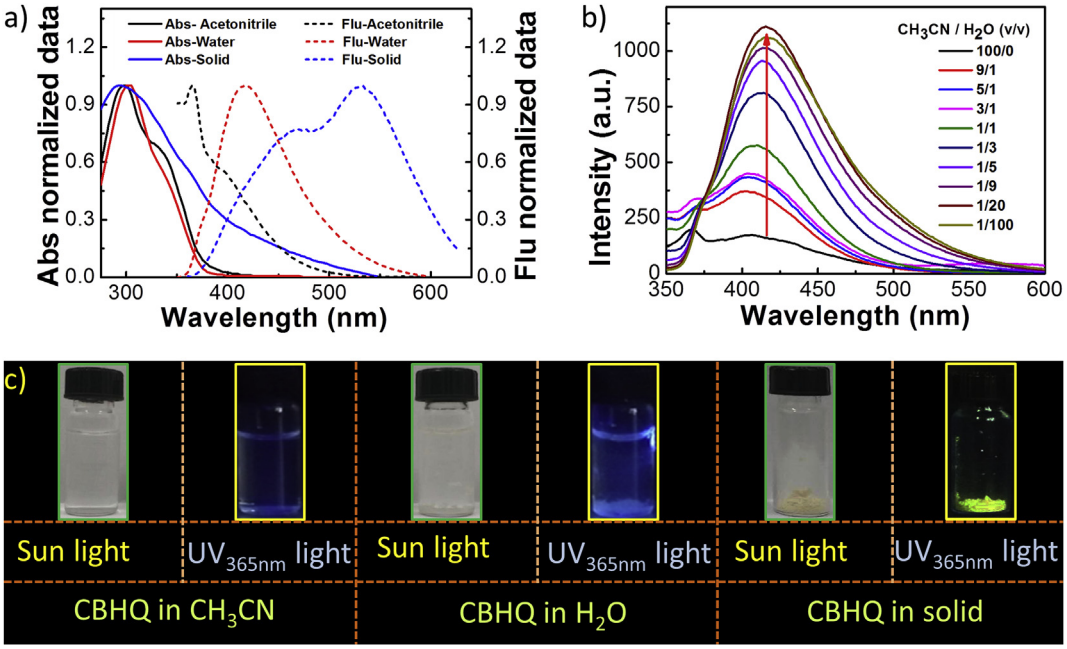

Fig. 1. (a) Normalized UV absorption and fluorescence emission spectra of probe CHBQ (1×10^{-5} mol/L) in CH_3CN, H_2O and solid ($\lambda_{ex} = 330$ nm); (b) Fluorescence emission spectrum of probe CHBQ (1×10^{-5} mol/L) in the mixture solvent of CH_3CN and H_2O with different volume ratio ($\lambda_{ex} = 330$ nm); (c) The photographs of CHBQ in CH_3CN, H_2O and solid under sun light and $UV_{365\ nm}$ lamp.

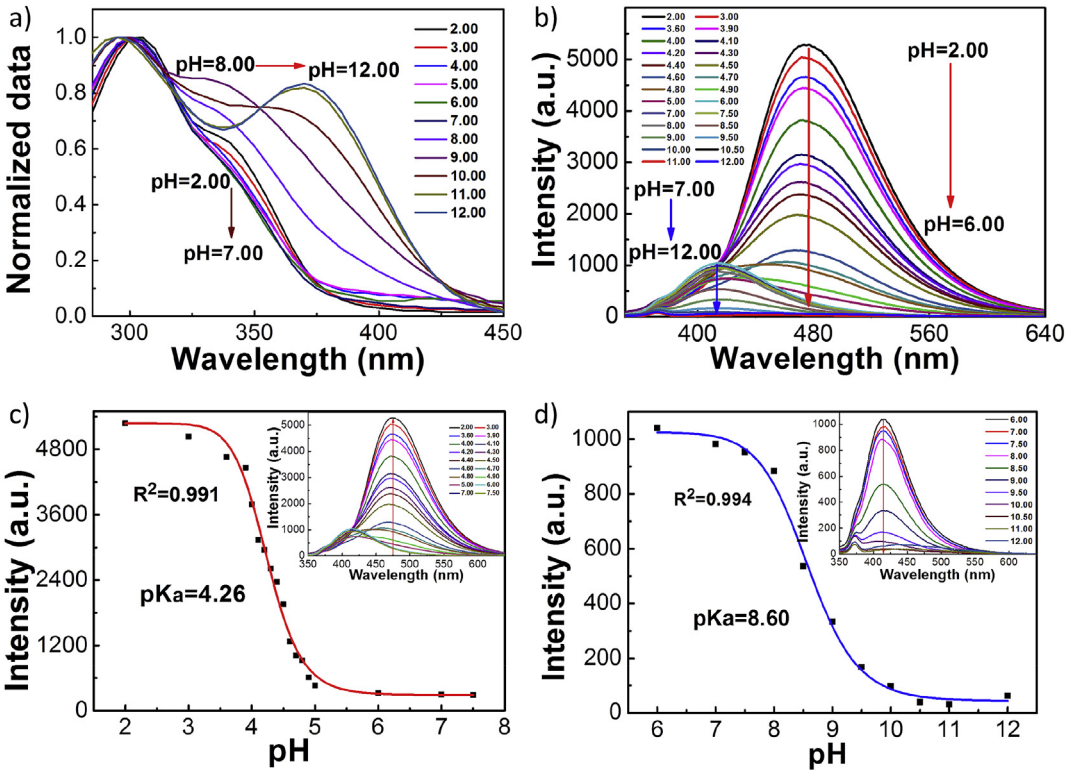

Fig. 2. The UV absorption (a) and fluorescence emission spectra (b) of CHBQ (1×10^{-5} mol/L) in different pH. Sigmoidal fitting of the pH-dependent emission of probe CHBQ (1×10^{-5} mol/L) in 475 nm (c) and 415 nm (d) ($\lambda_{ex} = 330$ nm). Insert: fluorescence emission titration spectra of CHBQ in acid (c) and alkali (d).

titration platforms was changed about 23 times and 21 times in acid and alkali, respectively. The titration results implied that there was a good sensitivity for probe CHBQ to detect a broad range pH.

3.4. Reversibility, interference and time course test

The reversibility of the probe represents the value of the probe in practical applications, we performed a reversibility experiment of the probe CHBQ (1×10^{-5} mol/L) between pH 4.00-7.00 and pH 7.00-10.00 in the mixed solution of acetonitrile-water (1/99, v/v). As shown in Fig. 3, the probe is still able to recover the fluorescence intensity at pH 4.00 ($\lambda = 475$ nm) and pH 10.00 ($\lambda = 415$ nm) after five cycles, which indicated the probe with a good reversibility.

Because the actual samples are complicated for the fact that there may be a variety of ions including some metal ions and anions in samples, so it is very important for the probe CHBQ to conduct the interference experiments for pH detection. The interference test of the probe CHBQ (1×10^{-5} mol/L) for pH detection was carried out in potassium hydrogen phthalate (pH = 4.00) and sodium tetrabrate (pH = 9.18) buffer solution. The interfering ions (1×10^{-4} mol/L) include K^+, Ca^{2+}, Na^+, Mg^{2+}, Al^{3+}, Zn^{2+}, Fe^{3+}, Fe^{2+}, Cu^{2+}, Ag^+, Pb^{2+}, Cr^{2+}, Cd^{2+}, Co^{2+}, Ni^{2+}, Mn^{2+}, F^-, Cl^-, Br^-, I^-, CO_3^{2-}, HCO^{3-}, CH_3COO^-, NO_3^-, NO_2^-, SO_4^{2-}, SO_3^{2-}, $S_2O_3^{2-}$, $H_2PO_4^-$, HPO_4^{2-}, ClO_4^-, S^{2-}. As shown in Fig. 3c, in the pH 9.18 buffer solution, the detection of pH by probe CHBQ is hardly affected by other ions. In the buffer solution with pH 4.00, most of the ions have no significant effect on the pH detection, only the excess Fe^{3+} reduced the fluorescence of probe CHBQ at pH 4.00 by about 20%, which indicating that the probe has good anti-interference ability for pH detection.

In addition, the time-response of the probe CHBQ for pH detection was also measured to investigate the detection response time. After the probe CHBQ (1×10^{-5} mol/L) was uniformly mixed with the calibrated solution of pH 4.00 and pH 10.00, the fluorescence curve was measured every 30 s. As shown in Fig. 3d, the fluorescence intensity of the probes CHBQ reached a stable level after CHBQ mixed with pH solution for 30 s, which indicated that the probe CHBQ is a high-efficiency pH detection probe.

3.5. Proposed mechanism and theoretical calculations

According to the above experimental phenomena and other reported literatures [32,41,42], the broad pH response mechanism of CHBQ we proposed is as follows. When CHBQ dissolved in acetonitrile, the N, N′-diformylhydrazine bond can rotate randomly, which decrease the fluorescence emission. It is well accepted that the N, N′-diformylhydrazine bond can produce an isomerization similar to the enol conversion of the enol in high polar solvents [41]. We infer that the isomerized N, N′-diformylhydrazine bond could occur and simultaneously triggered excited-state intramolecular proton transfer (ESIPT) process forming a six membered ring when CHBQ dispersed in water (Fig. 4a), which hindered the random rotation of CHBQ backbone and enhanced fluorescence emission. Moreover, when acid added in CHBQ, the N atom in quinoline and −C=N− bond will be protonated and a new five-membered ring will be formed between the protonated quinoline and O due to the presence of hydrogen bond [32]. This change causes the CHBQ backbone become more rigid and shows strongest fluorescence emission. In addition, after CHBQ was protonated, the lone pair electrons at the N atom of quinoline and −C=N− bond disappeared, and the pull electron capacity of the quinoline moiety increased. This change will lead to ICT process that the electron transfer from coumarin moiety to quinoline moiety will occur in CHBQ. Therefore, when pH changes from 7.00 to 2.00, the UV absorption peak about 330 nm produces a weak red shift, and the fluorescence produces a red shift of about 60 nm. Meanwhile, due to the presence of AIE effect in CHBQ, the fluorescence at about

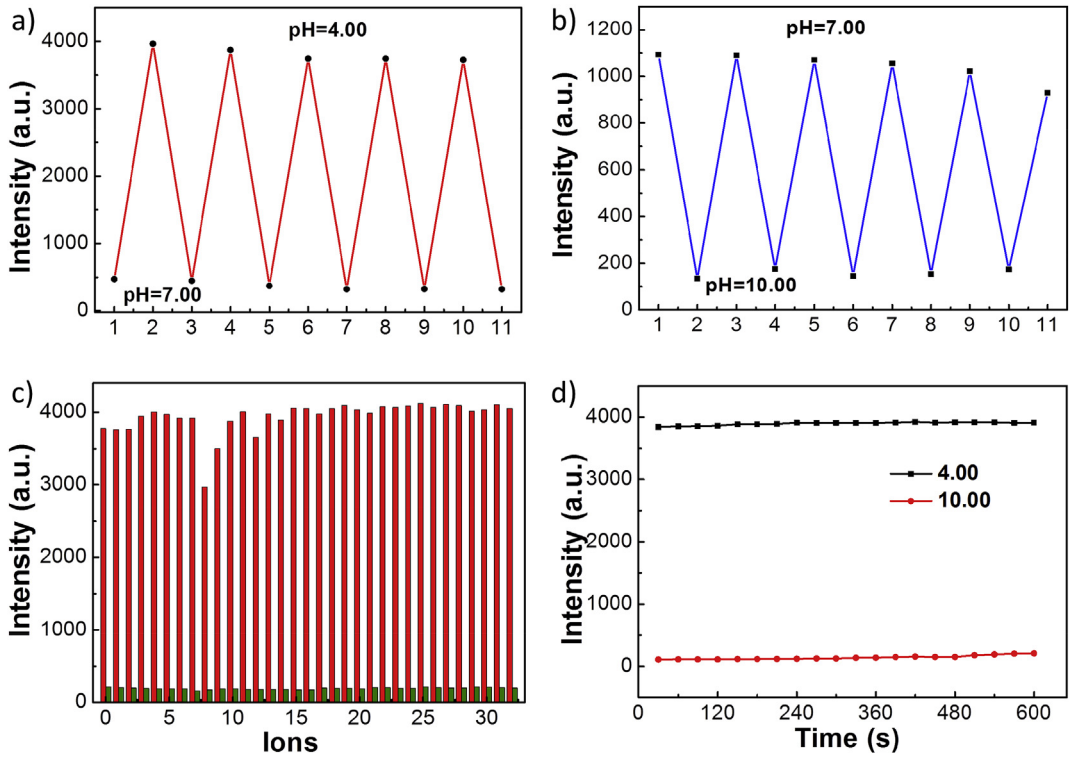

Fig. 3. Fluorescence intensity reversible changes of CHBQ (1×10^{-5} mol/L) at 475 nm between pH 4.00 and 7.00 (a) and at 415 nm between pH 10.00 and 7.00 (b) ($\lambda_{ex} = 330$ nm) in CH_3CN-H_2O (1/99, v/v) system. (c) Fluorescence responses of CHBQ (1×10^{-5} mol/L) in mixed solution of CH_3CN-H_2O (1/99, v/v) at pH 4.00 (475 nm) and pH 9.18 (415 nm) in the presence of diverse ions (1×10^{-4} mol/L), respectively ($\lambda_{ex} = 330$ nm). 0, blank; 1, K^+; 2, Ca^{2+}; 3, Na^+; 4, Mg^{2+}; 5, Al^{3+}; 6, Zn^{2+}; 7, Fe^{3+}; 8, Fe^{2+}; 9, Cu^{2+};10, Ag^+; 11, Pb^{2+}; 12, Cr^{2+}; 13, Cd^{2+}; 14, Co^{2+}; 15, Ni^{2+}; 16, Mn^{2+}; 17, F^-; 18, Cl^-; 19 Br^-; 20, I^-; 21, CO_3^{2-}; 22, HCO_3^-; 23, CH_3COO^-; 24, NO_3^-; 25, NO_2^-; 26, SO_4^{2-}; 27, SO_3^{2-}; 28, $S_2O_3^{2-}$; 29, $H_2PO_4^-$; 30, HPO_4^{2-}; 31, ClO_4^-; 32, S^{2-}; red bar: pH = 4.00; blue bar: pH = 9.18. (d) The fluorescence change of CHBQ with time at pH = 4.00 ($\lambda_{em} = 475$ nm) and at pH = 10.00 ($\lambda_{em} = 415$ nm).

475 nm gradually increases. When probe CHBQ is in alkali, the hydrazine moiety is deprotonated, the charge is transferred to O atom, thus increasing the π-conjugation length of the molecule. Consequently, when the pH changes from 8.00 to 12.00, the absorption peak produced a red shift about 40 nm. At the same time, due to the presence of negative charge, the hydrophilicity of the probe CHBQ increases, thereby the aggregation state is destroyed, the fluorescence decreased. The change of ^{1}HNMR of CHBQ in acetonitrile, acid and alkaline (Fig. S5) also indicated that there are different structures when the probe CHBQ presented in different solvents.

To demonstrate the existence of ICT properties in acidified CHBQ, the fluorescence emission spectra of acidified CHBQ (1×10^{-5} mol/L) containing 20 μL CF_3COOH in 2 mL different solvents were investigated. As shown in Fig. S6b, the maximum emission peaks of CHBQ solution are gradually red-shifted as the increase of solvent polarity. In contrast, the fluorescence spectra of CHBQ in neutral solvent (Fig. S6a) and alkaline solution (Fig. S6c) has little change with increasing of solvent polarity, indicating the weak ICT characteristics.

3.6. Theoretical structure simulation

In order to better understand the structure changes of probe CHBQ, the DFT calculation was used to simulate the structure of the probe CHBQ under different conditions, where B3LYP/6-31G (d) level was chose as basic set. As shown in Fig. 4b, the LUMO electron cloud of CHBQ in acetonitrile is mainly concentrated in the coumarin moiety, and the HOMO electron cloud is mainly concentrated in quinoline moiety. The electron cloud distribution of LUMO and HOMO of CHBQ under alkaline conditions is similar to that of acetonitrile. In water, the electron cloud of LUMO and HOMO don't change significantly except for expanding to the hydrazide bond. In acid, LUMO electron cloud expands to the whole molecular, and HOMO electron cloud transfers to the coumarin unit. The energy band-gaps between the HOMO and LUMO energy levels in acetonitrile, water, acid and alkaline were calculated as 3.59 eV, 3.40 eV, 3.95 eV and 3.03 eV, respectively. The measured band-gaps were calculated from the extrapolation of the absorption edges and the equation $E_g = 1240/\lambda$ in acetonitrile, water, acid and alkaline was 3.31 eV, 3.26 eV 3.29 eV and 2.90 eV. The similar Eg results of experiment and theoretical calculations confirmed that the proposed action mechanism, which is consistent with the actual molecular structural changes.

3.7. Test paper strips of CHBQ for pH detection

The simple detection device of broad range pH in real life is of great significance. On account of that the probe CHBQ could response pH at different wavelength with the same excitation wavelength. Based on the case, test paper strips of CHBQ for pH detection were developed. As seen from Fig. 5, when the acidic solution was added to the paper strips containing CHBQ, the color of the strips is cyan under the $UV_{365\ nm}$ lamp. As the pH increase, the color of the paper strips turned to blue. When the pH of the solution continues to increase, the blue fluorescence of the paper strips gradually decreases, which can be observed by naked eyes under $UV_{365\ nm}$ lamps. Besides, the test paper strips could be used to detect volatilized solvent such as acetic acid and ethylenediamine. Due to the gas from the solvent interacted with CHBQ, the color of test paper above acetic acid and ethylenediamine changed to cyan and darken under $UV_{365\ nm}$ lamp respectively.

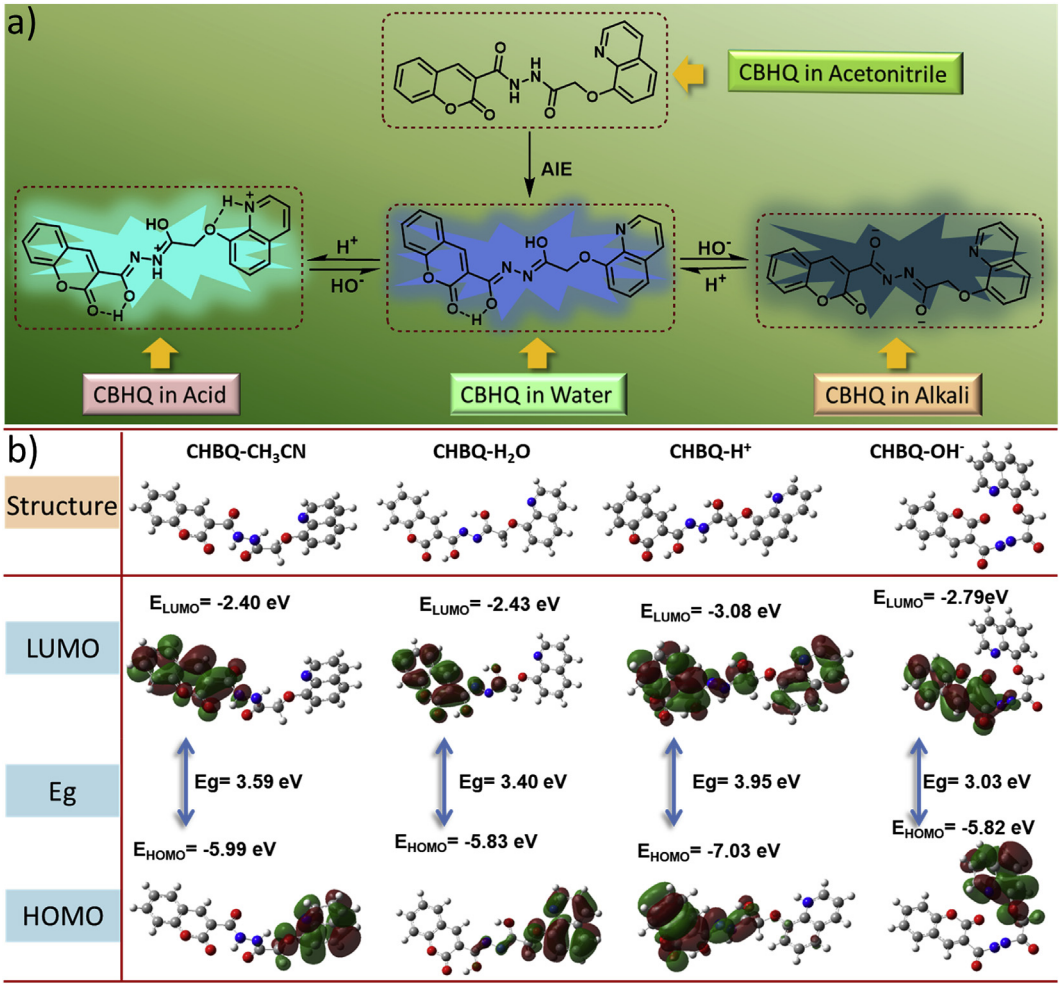

Fig. 4. (a) Structure changes of probe CHBQ in CH_3CN, H_2O, acid and alkali; (b) Theoretical simulation and electron cloud distribution of probe CHBQ in CH_3CN, H_2O, acid and alkali.

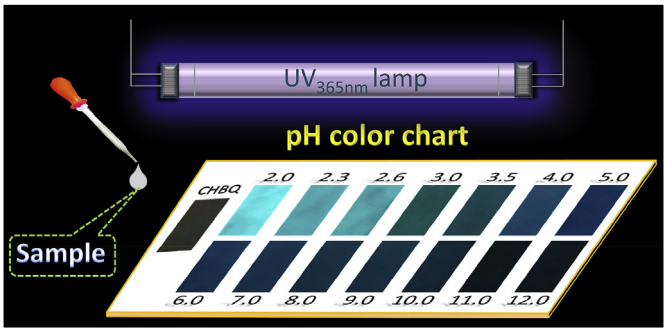

Fig. 5. The pH sensor trips containing CHBQ under $UV_{365\ nm}$ lamp.

The PL data of solid, CIE diagram and CIE coordinates of CHBQ in different pH were showed on Fig. S7 and Fig. S8. When pH changed from 2.00 to 5.00, the fluorescence of solid CHBQ at about 480 nm decreased and the maximum wavelength took place blue-shift gradually. And in CIE diagram, the coordinate of CHBQ in pH 2.00 is (0.183, 0.271), which was located in cyan area. When pH changed from 2.00 to 5.00, the color in CIE diagram varied from the cyan area to the blue area. When pH was 6.00, the coordinate of CHBQ is (0.148, 0.041), which was located in blue area. When pH changed from 6.00 to 12.00, the fluorescence of CHBQ at about 415 nm decreased gradually, and the color in CIE diagram all in blue area. All of these indicate that CHBQ is a satisfactory pH-responsive fluorescent probe.

4. Conclusion

Combining the characteristics of pH probes and the mechanism of AIE molecules, we have rationally designed and synthesized a probe CHBQ. The probe CHBQ exhibited fascinating photophysical properties. When probe CHBQ was in acetonitrile, there was a weak fluorescence emission peak at about 405 nm. In the mixed solution of acetonitrile and water, the fluorescence of probe CHBQ at 415 nm gradually enhanced as the proportion of water increased. At the excitation of 330 nm, the probe CHBQ shows different fluorescence changes from pH 2.00 to pH 12.00. Under acidic conditions, the fluorescence emission peak of the probe CHBQ gradually decreased and presented a blue shift from 475 nm to 415 nm as the pH changes from 2.00 to 6.00. Meanwhile, the color change of CHBQ solution from cyan to blue will be observed under $UV_{365\ nm}$ lamp. Under alkaline conditions, as the pH changes from 7.00 to 12.00, the fluorescence emission peak of the probe CHBQ at 415 nm gradually decreased, and the blue color of the solution gradually darkens under $UV_{365\ nm}$ lamp. The response time for probe CHBQ detection of pH was fast as 30 s and hardly interfered by other ions. In addition, CHBQ could be developed as a pH test strip for the detection of a broad range pH in actual samples.

Declaration of Competing Interest

The authors declare that they have no known competing financial interests or personal relationships that could have appeared to influence the work reported in this paper.

Acknowledgments

The work described in this paper was supported by the National Natural Science Foundation of China (No.21601111, 21571116 and 21807067), the Youth Science Foundation of Shanxi Province (No.201601D021054), Program for the Outstanding Innovative Teams of Higher Learning Institutions of Shanxi (2017−07) and SanJin Scholars Support Plan under Special Funding (2017−06). We also thank the Scientific Instrument Center of Shanxi University for assistance during the characterizations of the compounds.

Appendix A. Supplementary data

Supplementary data to this article can be found online at https://doi.org/10.1016/j.saa.2019.117650.

References

[1] Z. Yang, W. Qin, J.W.Y. Lam, S. Chen, H.H.Y. Sung, I.D. Williams, B. Tang, Fluorescent pH sensor constructed from a heteroatom containing luminogen with tunable AIE and ICT characteristics, Chem. Sci. 4 (2013) 3725−3730.
[2] Q. Feng, Y. Li, L. Wang, C. Li, J. Wang, Y. Liu, K. Li, H. Hou, Multiple-color aggregation-induced emission (AIE) molecules as chemodosimeters for pH sensing, Chem. Commun. 52 (2016) 3123−3126.
[3] X. Liu, J. Han, Y. Zhang, X. Yang, Y. Cui, G. Sun, A novel pH probe based on ratiometric fluorescent properties of dicyanomethylene-4H-chromene platform, Talanta 174 (2017) 59−63.
[4] J. Qiu, S. Jiang, H. Guo, F. Yang, An AIE and FRET-based BODIPY sensor with large Stoke shift: novel pH probe exhibiting application in CO_3^{2-} detection and living cell imaging, Dyes Pigments 157 (2018) 351−358.
[5] V. Wagner, M. Chytrý, D. Zelený, H. Wehrden, A. Brinkert, J. Danihelka, N. Hölzel, F. Jansen, J. Kamp, P. Lustyk, K. Merunková, S. Palpurina, Z. Preislerová, K. Wesche, Regional differences in soil pH niche among dry grassland plants in Eurasia 126 (2017) 660−670.
[6] Q. Ma, X. Cao, Y. Xie, Y. Gu, Y. Feng, W. Mi, X. Yang, l. Wu, Regional differences in soil pH niche among dry grassland plants in Eurasia, Environ. Exp. Bot. 133 (2017) 139−150.
[7] W. Zhu, J. Niu, D. He, Y. Sun, Y. Xu, J. Ge, Near-infrared pH probes based on phenoxazinium connecting with nitrophenyl and pyridinyl groups, Dyes Pigments 149 (2018) 481−490.
[8] Y. Yue, F. Huo, S. Lee, C. Yin, J. Yoon, A review: the trend of progress about pH probes in cell application in recent years, Analyst 142 (2017) 30−41.
[9] H. Wang, T. Kang, X. Wang, L. Feng, A facile strategy for achieving high selective Zn(II) fluorescence probe by regulating the solvent polarity, Talanta 184 (2018) 7−14.
[10] H. Wang, T. Kang, X. Wang, L. Feng, Design and synthesis of a novel tripod rhodamine derivative fortrivalent metal ions detection, Sens. Actuators, B 264 (2018) 391−397.
[11] L. Feng, L. Guo, X. Wang, Preparation,properties and applications in cell imaging and ions detection of conjugated polymer nanoparticles with alcoxyl bonding fluorenecore, Biosens. Bioelectron. 87 (2017) 514−521.
[12] J. Ge, L. Fan, K. Zhang, T. Ou, Y. Li, C. Zhang, C. Dong, S. Shuang, S. Wong, A two-photon ratiometric fluorescent probe for effective monitoring of lysosomal pH in live cells and cancer tissues, Sens. Actuators, B 262 (2018) 913−921.
[13] S. Shen, X. Zhang, Y. Ge, Y. Zhu, X. Lang, X. Cao, A near-infrared lysosomal pH probe based on rhodamine derivative, Sens. Actuators, B 256 (2018) 261−267.
[14] F. Wang, D. Liu, Y. Shen, J. Liu, X. Tian, Q. Zhang, J. Wu, S. Li, Y. Tian, A two-photon mitochondria-targeted fluorescent probe for the detection of pH fluctuation in tumor and living cells, Dyes Pigments 166 (2019) 92−97.
[15] W. Zhang, L. Fan, Z. Li, T. Ou, H. Zhai, J. Yang, C. Dong, S. Shuang, Thiazole-based ratiometric fluorescence pH probe with large Stokesshift for intracellular imaging, Sens. Actuators, B 233 (2016) 566−573.
[16] J. Chao, Y. Liu, J. Sun, L. Fan, Y. Zhang, H. Tong, Z. Li, A ratiometric pH probe for intracellular pH imaging, Sens. Actuators, B 221 (2015) 427−433.
[17] M. Liu, Y. Lv, X. Jie, Z. Meng, X. Wang, J. Huang, A. Peng, Z. Tian, A super-sensitive ratiometric fluorescent probe for monitoring intracellular subtle pH fluctuation, Sens. Actuators, B 273 (2018) 167−175.
[18] Y. Cai, C. Gui, K. Samedov, H. Su, X. Gu, S. Li, An acidic pH independent piperazine−TPE AIEgen as a unique bioprobe for lysosome tracing, Chem. Sci. 8 (2017) 7593−7603.
[19] Z. Zhou, F. Gu, L. Peng, Y. Hu, Q. Wang, Spectroscopic analysis and in vitro imaging applications of a pH responsive AIE sensor with a two-input inhibit function, Chem. Commun. 51 (2015) 12060−12063.
[20] D. Li, Y. Zhang, Z. Fan, J. Chen, J. Yu, Coupling of chromophores with exactly opposite luminescence behaviours in mesostructured organosilicas for high-efficiency multicolour Emission, Chem. Sci. 6 (2015) 6097−6101.
[21] J. Qian, B. Tang, AIE luminogens for bioimaging and theranostics: from organelles to animals, Chem 3 (2017) 56−91.
[22] J. Liu, C. Zhang, J. Dong, J. Zhu, C. Shen, G. Yang, X. Zhang, Endowing a triarylboron compound showing ACQ with AIE characteristics by transforming its emissive TICT state to be dark, RSC Adv. 7 (2017) 14511−14515.
[23] J. Luo, Z. Xie, J.W. Lam, L. Cheng, H. Chen, C. Qiu, H. Kwok, X. Zhan, Y. Liu, D. Zhu, B. Tang, Aggregation-induced emission of 1-methyl-1,2,3,4,5- pentaphenylsilole, Chem. Commun. 18 (2001) 1740−1741.
[24] X. Wang, Q. Jiang, Y. Man, S. Feng, Y. Lee, H. Liu, A novel amphiphilic pH-responsive AIEgen for highly sensitivedetection of protamine and heparin, Sens. Actuators, B 261 (2018) 233−240.
[25] P. Shen, Z. Zhuang, Z. Zhao, B. Tang, AIEgens based on main group Heterocycles, J. Mater. Chem. C 6 (2018) 11835−11852.
[26] J. Zhao, Z. Chi, Y. Zhang, E. Ubba, Z. Chi, Recent progress in the mechano-fluorochromism of distyrylanthracene derivatives with aggregation-induced emission, Mater. Chem. Front. 9 (2018) 1595−1608.
[27] Y. Hong, J.W. Lam, B. Tang, Aggregation-induced emission: phenomenon, mechanism and applications, Chem. Commun. 29 (2009) 4332−4353.
[28] R. Hu, N.L. Leung, B. Tang, AIE macromolecules: syntheses, structures and functionalities, Chem. Soc. Rev. 43 (2014) 4494−4562.
[29] S. Chen, M. Zhao, J. Su, Q. Zhang, X. Tian, S. Li, H. Zhou, J. Wu, Y. Tian, Two novel two-photon excited fluorescent pH probes based on the Ap-D-p-A system for intracellular pH mapping, Dyes Pigments 136 (2017) 807−816.
[30] J. Ma, W. Li, J. Li, R. Shi, G. Yin, R. Wang, A small molecular pH-dependent fluorescent probe for cancer cell imaging in living cell, Talanta 182 (2018) 464−469.
[31] B. Tang, F. Yu, P. Li, L. Tong, X. Duan, T. Xie, X. Wang, A near-infrared neutral pH fluorescent probe for monitoring minor pH changes: imaging in living HepG2 and HL-7702 cells, J. Am. Chem. Soc. 131 (2009) 3016−3023.
[32] G. Li, D. Zhu, L. Xue, H. Jiang, Quinoline-based fluorescent probe for ratiometric detection of lysosomal pH, Org. Lett. 15 (2013) 5020−5023.
[33] W. Huang, W. Lin, X. Guan, Development of ratiometric fluorescent pH sensors based on chromenoquinoline derivatives with tunable pKa values for bioimaging, Tetrahedron Lett. 55 (2014) 116−119.
[34] C. Wang, C. Li, X. Wu, A. Pettman, J. Xiao, pH-regulated asymmetric transfer Hydrogenation of quinolines in water, Angew. Chem. 121 (2009) 6646−6650.
[35] N.I. Georgiev, A.I. Said, R.A. Toshkova, R.D. Tzoneva, V.B. Bojinov, A novel water-soluble perylenetetracarboxylic diimide as a fluorescent pH probe: chemosensing, biocompatibility and cell imaging, Dyes Pigments 160 (2019) 28−36.
[36] T. Myochin, K. Kiyose, K. Hanaoka, H. Kojima, T. Nagano, Rational design of ratiometric near-infrared fluorescent pH probes with various pKa values, based on aminocyanine, J. Am. Chem. Soc. 133 (2011) 3401−3409.
[37] Q. Lin, X. Zhu, Y. Fu, Q. Yang, B. Sun, T. Wei, Y. Zhang, Rationally designed supramolecular organogel dual-channel sense F^-under gelegel states via ion-controlled AIE, Dyes Pigments 113 (2015) 748−753.
[38] D. Xu, M. Liu, H. Zou, J. Tian, H. Huang, Q. Wan, Y. Dai, Y. Wen, X. Zhang, Y. Wei, A new strategy for fabrication of water dispersible and biodegradable fluorescent organic nanoparticles with AIE and ESIPT characteristics and their utilization for bioimaging, Talanta 174 (2017) 803−808.
[39] S. Samanta, S. Goswami, M.N. Hoque, A. Ramesh, G. Das, An aggregation-induced emission (AIE) active probe renders Al(III) sensing and tracking of subsequent interaction with DNA, Chem. Commun. 50 (2014) 11833−11836.
[40] V. Kachwal, I.S. Krishna, L. Fageria, J. Chaudhary, R.K. Roy, R. Chowdhury, I.R. Laskar, Exploring the Hidden potential of a benzothiazolebased schiff-base exhibiting AIE and ESIPT and its activity in pH sensing, intracellular imaging and ultrasensitive & selective detection of aluminium (Al^{3+}), Analyst 143 (2018) 3741−3748.
[41] L.G. Chekanova, A.V. Radushev, A.E. Lesnov, E.A. Sazonova, Physicochemical properties of 1,2-diacylhydrazines derived from aliphatic carboxylic acids, Russ. J. Gen. Chem. 72 (2002) 1233−1237.
[42] M.A. Haque, L.J. Paliwal, Synthesis, spectral characterization and thermal aspects of coordination polymers of some transition metal ions with adipoyl bis(isonicotinoylhydrazone), J. Mol. Struct. 1134 (2017) 278−291.
[43] A.S. Islama, R. Bhowmicka, H. Mohammada, A. Katarkarb, M. Alia, A novel 8-Hydroxyquinoline-pyrazole based highly sensitive and selective Al(III) sensor in a purely aqueous medium with intracellular application: experimental and computational studies, New J. Chem. 40 (2016) 4710−4719.
[44] H.J. Yoon, M. Dakanali, D. Lichlyter, W.M. Chang, K.A. Nguyen, M.E. Nipper, M.A. Haidekker, E.A. Theodorakis, Synthesis and evaluation of self-calibrating ratiometric viscosity sensors, Org. Biomol. Chem. 9 (2011) 3530−3540.
[45] Z. Mao, L. Hu, C. Zhong, H. Zhang, B. Liu, Z. Liu, A dual-mechanism strategy to design a wide-range pH probe with multicolor fluorescence, Sens. Actuators, B 219 (2015) 179−184.